

# Dose Imaging Detectors for Radiotherapy Based on Gas Electron Multipliers

A.V. Klyachko<sup>a</sup>, D.L. Friesel<sup>b</sup>, C. Kline<sup>b</sup>, J. Liechty<sup>b</sup>, D.F. Nichiporov<sup>a</sup>, K.A. Solberg<sup>a</sup>

<sup>a</sup>Indiana University Cyclotron Operations, Bloomington, Indiana, USA

<sup>b</sup>PartTec, Ltd, Bloomington, Indiana, USA

---

## Abstract

New techniques in charged particle therapy and widespread use of modern dynamic beam delivery systems demand new beam monitoring devices as well as accurate 2D dosimetry systems to verify the delivered dose distribution. We are developing dose imaging detectors based on gas electron multipliers (GEM) with the goal of improving dose measurement linearity, position and timing resolution, and to ultimately allow pre-treatment verification of dose distributions and dose delivery monitoring employing scanning beam technology. A prototype 10x10 cm<sup>2</sup> double-GEM detector has been tested in the 205 MeV proton beam using electronic and optical readout modes. Preliminary results with electronic cross-strip readout demonstrate fast response and single-pixel (4 mm) position resolution. In optical readout mode, the line spread function of the detector was found to have  $\sigma=0.7$  mm. In both readout modes, the detector response was linear up to dose rates of 50 Gy/min, with adequate representation of the Bragg peak in depth-dose profile measurements.

**Key words:** GEM detector; hadron therapy; dose imaging

---

## 1. Introduction

New methods of beam delivery in charged particle therapy such as beam scanning and energy stacking are becoming increasingly popular as more new clinical proton facilities include Intensity Modulated Proton Therapy (IMPT) in their specifications. Promising better coverage of clinical targets with dose fields, the IMPT technology implies dynamic variations in beam's lateral position, intensity and energy during the beam delivery. A typical radiotherapy treatment delivers about 2 Gy of absorbed dose into a ~1 liter target volume and, implemented with an IMPT technique, will require ~10,000 individual beams delivered in about 100 seconds, i.e. ~100 Hz spot delivery frequency or, with re-scanning, even ~300 Hz. To control the dose in each spot to better than 5% on a daily basis, one requires a readout and feedback system with a response time of ~0.1 ms. Dose distributions created in IMPT are characterized by high lateral and depth dose gradients. Verification of such fields therefore requires accurate measurements of lateral and depth dose profiles as well as absorbed dose. Main requirements for a beam monitor are: response time ~0.1 ms, position resolution of 1-2 mm, and dose measurement linearity ~1%. For a dose verification detector, sub-millimeter spatial resolution and tissue-equivalence of the dose response are desirable.

Existing detectors and measurement techniques used in the clinical practice of proton therapy are not well suited for dynamic dose distribution monitoring. Solutions exist, but as one-of-a-kind, experimental systems [1, 2, 3]. The difficulties with monitoring and dose verification in IMPT could be resolved by implementation of gaseous amplification devices, such as the Gas Electron Multiplier (GEM) [4]. GEMs offer fast performance, robustness and flexibility in the detector de-

sign, allowing for both electronic and optical readout schemes. Recently, the results of characterization of scintillating GEM detectors, developed for pre-treatment dose distribution verification in particle therapy, has been reported for proton [5],  $\alpha$ -particle [6] and carbon [7] beams.

We are developing prototype GEM-based detectors for 2D dose imaging in radiotherapy with the goal of improving dose measurement linearity, position and timing resolution, and to ultimately allow pre-treatment verification of dose distributions and dose delivery monitoring employing scanning beam technology. In the present work, we report on the first results obtained in detector prototype tests using a 200 MeV proton beam.

## 2. Materials and methods

### 2.1. Detector setup, electronic readout

The detector, schematically shown in Fig. 1, consists of a double-GEM amplification structure with a copper-clad Kapton cathode and a crossed-strip collector electrode, mounted in an air-tight aluminum housing with thin 87x81 mm<sup>2</sup> stainless steel windows, continuously flushed with an Ar/CO<sub>2</sub> (70/30%) gas mixture. The 100x100 mm<sup>2</sup> GEM foils produced by Tech-Etch [8] have a triangular hole pattern with equidistant holes at a pitch of 140  $\mu$ m and hole diameters in the metal layers of 70  $\mu$ m. The GEMs were mounted on 2.4 mm thick Rexolite frames. The multi-layer two-dimensional strip anode with 340  $\mu$ m wide Y-strips (lower layer) and 80  $\mu$ m wide X-strips (upper layer), both at 400  $\mu$ m pitch, is similar in design to the COMPASS [9] readout electrode. It was also produced by Tech-Etch. Groups of 10 narrow strips were connected together to form 4 mm wide anodes providing a 4x4 mm<sup>2</sup> readout pixel size. A 12x13 array

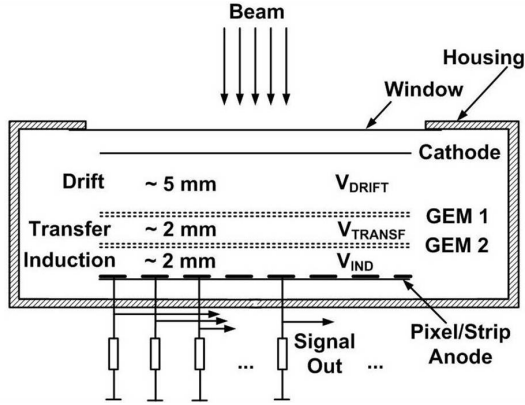


Figure 1: Schematic diagram of the detector setup in electronic readout mode.

of strips was read out using gated integrator cards, developed at the Indiana University Cyclotron Facility (IUCF), and a VME-based data acquisition system. During the beam measurements, the GEM<sub>1</sub> and GEM<sub>2</sub> were operated at 350 V and 340 V, respectively, with the drift, transfer and induction fields set respectively at 1.5 kV/cm, 1.7 kV/cm and 1.7 kV/cm, each stage being powered from an individual power supply.

## 2.2. Detector setup, optical readout

The same detector housing, cathode and double-GEM amplification structure were used in the optical readout mode, as shown in Fig. 2. The stainless steel windows were replaced by aluminized Mylar entrance and transparent Mylar exit windows. The strip anode was removed and the bottom copper layer of GEM<sub>2</sub> served as a charge collector electrode, its signal was read out by a IUCF-designed recycling integrator card. The detector volume was continuously flushed with an Ar/CF<sub>4</sub> (95/5%) gas mixture. Both GEMs were operated at 300 V, with the same drift and transfer fields as described in Section 2.1. The light produced by the electron avalanches was detected by an SBIG ST-6 astronomical camera with thermoelectric cooling from the Santa Barbara Instrument Group [10] and a Tamron CCTV CS zoom lens. The camera was positioned away from the beam and was shielded with lead and concrete blocks to reduce radiation damage to the CCD sensor. The light path was enclosed in light-tight shielding made from a black aluminum foil. The Texas Instruments TC-241 CCD sensor, with a quantum efficiency of 62% at 650 nm, is well matched to the emission spectrum of the Ar/CF<sub>4</sub> gas mixture [11]. The sensor has 375x241 pixels with dimensions of 23x27  $\mu\text{m}^2$ , which translates to 0.36x0.42 mm<sup>2</sup> at the GEM<sub>2</sub> location. During the measurements, the camera was cooled to -30°C. The images were read out by the camera's native SBIG software and analyzed using SBIG and ImageJ software packages [12].

## 2.3. Experimental setup

The detector was tested in the IUCF Proton Dosimetry Test Facility with a 205 MeV proton beam. The experimental setup is shown in Fig. 3. The Ionization Chamber Beam Monitor (ICBM) was used to measure beam intensity and beam profile,

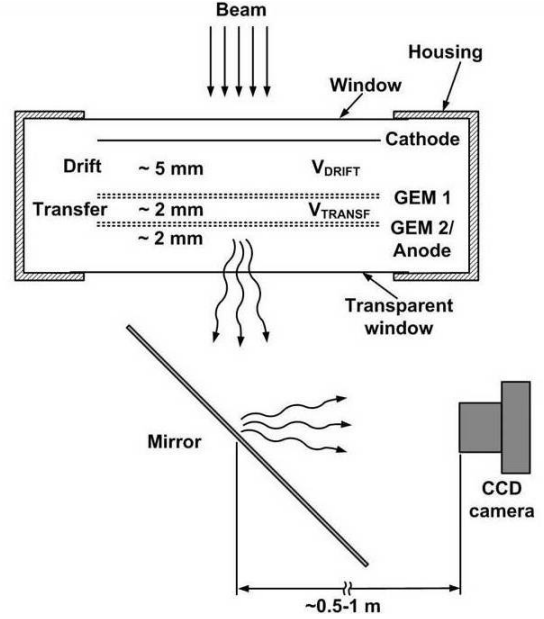


Figure 2: Schematic diagram of the detector setup in optical readout mode.

and to control the beam delivery, terminating the beam upon the delivery of a pre-set dose. The dose rate was varied by changing the beam current in the cyclotron. A 2.4 mm thick copper scatter foil spreaded the beam to about 6 cm diameter FWHM at the detector location, also degrading the beam energy to 198 MeV. For depth-dose measurements (see Section 3), the thickness of an acrylic phantom placed in front of the detector was varied by adding/removing acrylic sheets, with 1-10 mm steps. The dose linearity tests were carried out without any phantom material. Brass collimators were used to shape the beam impinging on the detector. A commercial Markus ionization chamber with NIST-traceable calibration in absorbed dose to water (PTW, Model TN23343) with a 5.3 mm diameter active area, positioned behind the detector, was used to estimate the dose rate.

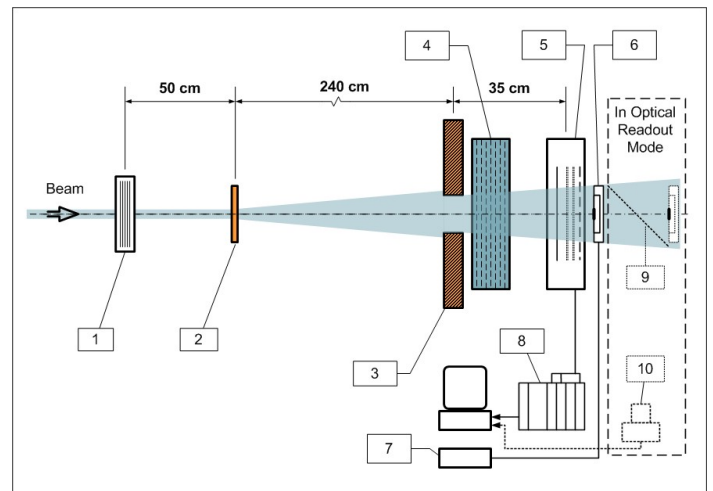


Figure 3: Schematics of the experimental setup. 1-ICBM; 2-scatter foil; 3-collimator; 4-acrylic phantom; 5-GEM detector; 6-Markus chamber; 7-therapy dosimeter/picoamperimeter; 8-VME DAQ; 9-mirror; 10-CCD camera.

## 2.4. Backgrounds and data analysis

In the electronic readout mode, the main sources of background are the noise pickup in the detector and in the cables. The background was measured before each beam measurement and subtracted from the data. In the optical readout mode, the main background sources are: a) camera offset; b) dark current (noise); c) ambient light. To take into account the backgrounds (a-c), an ambient light image was taken without beam and with the same exposure time as in beam measurements, and then subtracted from the images taken with the beam. Corrections for additional possible backgrounds (such as interactions of scattered beam and secondary particles with the camera's sensor, and scintillations in the detector gas and exit window caused by beam particles) were estimated at less than 1% total [5] and therefore were not applied. The images have been processed offline to correct for background and to remove extremely hot and cold isolated pixels, using the routines provided with the SBIG camera. The images then have been analyzed with ImageJ software to determine the light yield by integrating over an area of interest identical for all measurements.

## 3. Results and discussion

In the electronic readout mode, to estimate the position resolution of the detector, we performed series of measurements with different diameter collimators. The results obtained in the proton beam and with radioactive sources suggest that the spatial resolution is close to the single-pixel size, i.e. 4 mm. The dose-rate response has been measured with a 20 mm diameter collimator. The summed response of three X- and three Y-strips corresponding to the central part of the beam is shown in Fig. 4.

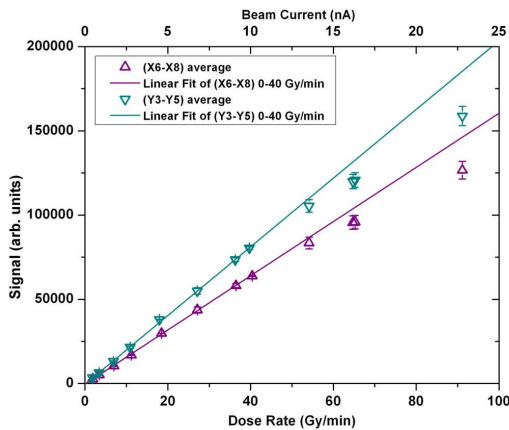


Figure 4: Dose-rate response of the detector in electronic readout mode. The lines are linear fits to the data below 40 Gy/min.

To evaluate the energy dependence of the detector's output, we measured the depth-dose response of the detector, with the beam current of about 6 nA corresponding to dose rate of  $\sim 12$  Gy/min without any material in the phantom, and up to  $\sim 40$  Gy/min at the Bragg peak. The depth-dose curves (summed response of six X- and six Y-strips) are shown in

Fig. 5. The curves are normalized to 1 at zero phantom thickness. The acrylic thickness is converted to water-equivalent depth. Note that the detector and the Markus chamber have sensitive areas of different size and both detect only a small (and different) portion of all particles coming out of the phantom, so one should not expect identical Bragg peaks from detector and Markus chamber. In future, we intend to increase the readout channel count and to use a wide aperture parallel plate ionization chamber instead of the Markus chamber for comparative measurements.

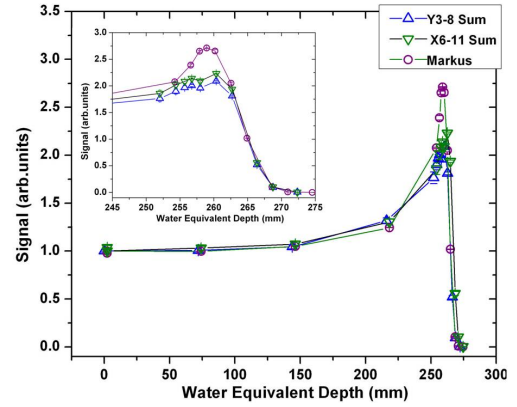


Figure 5: Depth-dose response of the detector in electronic readout mode. Insert: expanded view of the Bragg peak.

In the optical readout mode, collimators of different shapes were used to estimate the spatial resolution of the detector. An image of a  $1.4 \times 20$  mm<sup>2</sup> collimator obtained with 5 nA beam and 3 s exposure is shown in Fig. 6 (insert) together with the light intensity profile along a single-pixel line. The main peak has been fitted with a Gaussian curve with  $\sigma = 0.7$  mm. An

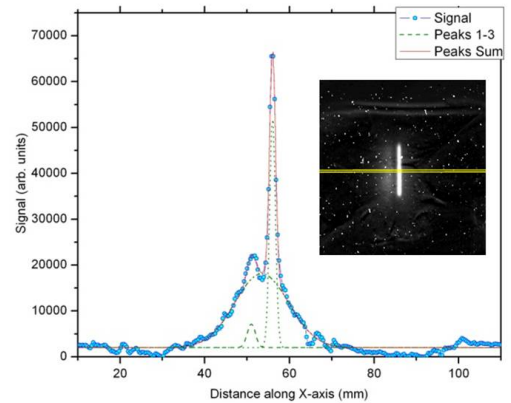


Figure 6: The  $1.4 \times 20$  mm<sup>2</sup> collimator image (insert) and the light intensity profile along the one-pixel wide horizontal line. The data are fitted with a superposition of 3 Gaussians.

image of a 20 mm diameter collimator is shown in Fig. 7 as well as a light intensity profile along a one-pixel wide line (insert). We attribute the  $\pm 3\%$  variations of intensity on the flattop to GEM gain non-uniformities caused by hole size variations. The detector dose-rate response in optical readout mode, mea-

sured with the same 20 mm diameter collimator, is shown in Fig. 8. Beam images were taken with 3 s exposures, shorter than the duration of the beam delivery. The depth-dose mea-

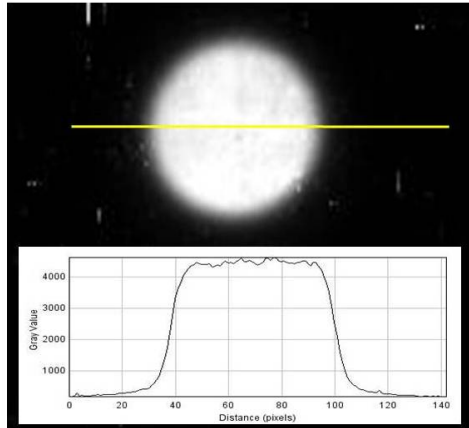


Figure 7: Top - an image of a 20 mm diameter collimator. Bottom - an image profile along the one-pixel wide horizontal line (shown in the upper part).

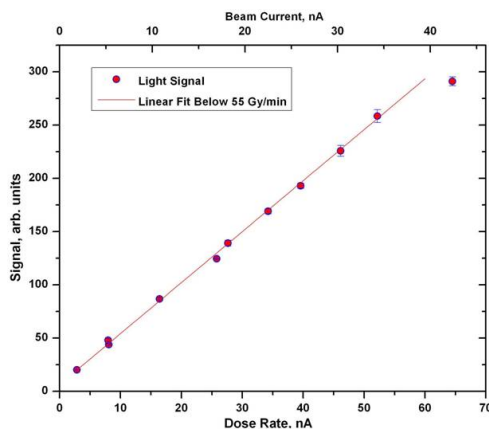


Figure 8: Dose rate response of the detector in optical readout mode. The line is a linear fit to the data below 55 Gy/min.

surements in the optical readout mode were carried out with a 50 mm diameter collimator and a beam current of 5 nA. Depth-dose curves, shown in Fig. 9, have been normalized to 1 at zero depth. At the peak, the charge signal exceeds the light signal by about 3.5%. One of the reasons for this might be the difference of the integration areas for charge and light signals.

#### 4. Conclusions

We have developed a prototype detector system for two-dimensional dose imaging in hadron therapy based on a double-GEM amplification structure, using either electronic or optical readout. In both modes, the detectors exhibit a linear dose rate response up to about 50 Gy/min and reproduce the Bragg peak in depth-dose measurements. In electronic readout mode, a position resolution of 4 mm (single-pixel) was observed. We expect that, using a multi-pad readout electrode with smaller pitch, the position resolution of the detector can be significantly

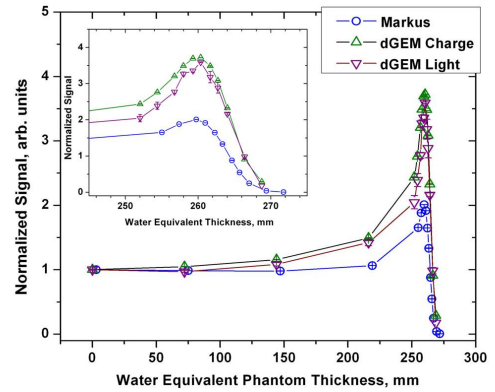


Figure 9: Bragg curves measured in optical readout mode. Compared are the light signal, the charge signal from the last GEM foil, and the Markus chamber signal. Insert - expanded view of the Bragg peak.

improved, at the cost of a significant increase in the number of readout channels. In the optical readout mode, the line spread function of the detector was found to have  $\sigma=0.7$  mm. The position resolution in this mode also can be improved by using a higher pixel count CCD camera.

The GEM-based detectors are promising candidates for the creation of two kinds of dosimetry systems: one, with electronic readout, would be a fast (timing resolution in the microsecond range), moderate spatial resolution (1-2 mm, limited by the cost of electronics) dose imaging detector for on-line scanning beam monitoring. Such a detector, with cross-strip readout, would also be a good candidate for low-rate applications, such as proton tomography. Another detector system, with optical readout, would be a slower, moderately priced detector with sub-millimeter spatial resolution suitable for the dose distribution verification and for quality assurance measurements in hadron therapy.

#### 5. Acknowledgements

The authors would like to thank Dr. V. Anferov and Dr. V. Derenchuk for support and assistance in carrying out the measurements with the proton beam, as well as for valuable discussions. This work was partially supported by NIH SBIR Grant 1R43CA13791-01A1.

#### References

- [1] J.M. Schippers et al, J. of Phys.: Conf. Ser. 41 (2006) 61.
- [2] M.T. Gillin et al, Med. Phys. 37 (2010) 154.
- [3] H.-J. Borchert et al, Nowotwory J. Oncol. 58 (2008) 62e.
- [4] F. Sauli, Nucl. Instr. and Meth. A 386 (1997) 531.
- [5] E. Seravalli et al, Phys.Med. Biol. 54 (2009) 3755.
- [6] E. Seravalli et al, IEEE Trans. Nucl. Sci. 54 (2007) 1271.
- [7] E. Seravalli et al, Phys.Med. Biol. 53 (2008) 4651.
- [8] Tech-Etch Corp, 45 Aldrin Rd, Plymouth, MA 02360.
- [9] C. Altunbas et al, Nucl. Instr. and Meth. A 490 (2002) 177.
- [10] Santa Barbara Instrument Group, 147-A Castilian Drive, Santa Barbara, CA 93117.
- [11] M.M.F.R. Fraga et al, Nucl. Instr. and Meth. A 504 (2003) 88.
- [12] W.S. Rasband, ImageJ, U. S. National Institutes of Health, Bethesda, Maryland, USA, <http://rsb.info.nih.gov/ij/>, 1997-2008.